

Singular diffraction-free surface plasmon beams generated by overlapping phase-shifted sources

Wang, Rong (EEE); Wei, Shibiao; Lin, Jiao; Wang, Qian; Yuan, Guanghui; Du, Luping; Xu, Le;
Hong, Minghui; Min, Changjun; Yuan, Xiaocong

2013

Wei, S., Lin, J., Wang, Q., Yuan, G., Du, L., Wang, R., et al. (2013). Singular diffraction-free surface plasmon beams generated by overlapping phase-shifted sources. *Optics Letters*, 38(7), 1182-1184.

<https://hdl.handle.net/10356/98721>

<https://doi.org/10.1364/OL.38.001182>

© 2013 Optical Society of America. This paper was published in *Optics Letters* and is made available as an electronic reprint (preprint) with permission of Optical Society of America. The paper can be found at the following official DOI: [<http://dx.doi.org/10.1364/OL.38.001182>]. One print or electronic copy may be made for personal use only. Systematic or multiple reproduction, distribution to multiple locations via electronic or other means, duplication of any material in this paper for a fee or for commercial purposes, or modification of the content of the paper is prohibited and is subject to penalties under law.

Downloaded on 23 Aug 2022 13:56:49 SGT

Singular diffraction-free surface plasmon beams generated by overlapping phase-shifted sources

Shibiao Wei,^{1,2} Jiao Lin,^{3,5} Qian Wang,² Guanghui Yuan,² Luping Du,² Rong Wang,^{1,2} Le Xu,⁴ Minghui Hong,⁴ Changjun Min,¹ and Xiaocong Yuan^{1,6}

¹*Institute of Modern Optics, Key Laboratory of Optical Information Science & Technology, Ministry of Education of China, Nankai University, Tianjin 300071, China*

²*School of Electrical & Electronic Engineering, Nanyang Technological University, Nanyang Avenue 639798, Singapore*

³*Singapore Institute of Manufacturing Technology, 71 Nanyang Drive 638075, Singapore*

⁴*Department of Electrical and Computer Engineering, National University of Singapore, 4 Engineering Drive 3 117576, Singapore*

⁵*e-mail: jiao_lin@scholars.a-star.edu.sg*

⁶*e-mail: xcyuan@nankai.edu.cn*

Received November 30, 2012; revised January 24, 2013; accepted February 14, 2013;
posted March 4, 2013 (Doc. ID 180956); published April 1, 2013

We propose and experimentally demonstrate the singular surface plasmon beam that presents a dark channel generated by a point dislocation and a long diffraction-free propagation distance up to $70\lambda_{\text{sp}}$. The singular surface beam is the result of the interference of two surface plasmon polariton (SPP) plane waves, which are launched by two coupling gratings with lateral displacement. An aperture-type near-field scanning optical microscope is used to map the intensity distribution of the singular SPP waves. The propagating point dislocation embedded in the beam is shown by full-wave calculations and is later verified by near-field interference in the experiment. © 2013 Optical Society of America

OCIS codes: 260.6042, 240.6680, 250.5403.

Surface plasmon polaritons (SPPs), electromagnetic surface waves tightly bound to the metal–dielectric interface, originate from the strong interaction between an external electromagnetic field and free-electron oscillations in metal [1]. Similar to free-space electromagnetic waves, unique optical properties of SPPs, such as focusing [2] and interference [3] arising from their intrinsic wave nature, have been demonstrated in recent years.

Phase singularity as another important concept in wave theory has received growing interest in SPPs. A phase singularity (dislocation) in an optical field refers to places where the phase of waves cannot be defined and the intensity vanishes at singularities. In free space, there are two types of dislocations: screw dislocation and edge dislocation [4]. A well-known example is optical vortices, laser beams with screw dislocations at the beam center, which have a spiral phase ramp surrounding the phase singularity. On the other hand, an edge dislocation is defined as a π phase jump across a line in the transverse plane of a laser beam. The Gauss–Hermite mode, e.g., $H_{1,0}$ in a laser, is a straightforward demonstration of an optical field with an edge dislocation, where a dark line can be found in the beam cross section [5]. Recently, plasmonic near-field distributions with screw dislocations have been generated either by a set of split curved slits [6] or by SPP interference or evanescent waves excited by free-space vortex beams on surfaces without structures [7,8]. In contrast to those existing in free-space vortex beams, the plasmonic screw dislocations do not propagate. Here, we introduce point dislocation in SPP waves as the counterpart of free-space edge dislocations. Both point and edge dislocations are propagating singularities that evolve into dark lines and surfaces in 2D and 3D spaces, respectively. The difference between an edge dislocation in a 3D space and a point dislocation is the direct consequence of dimensionality reduction. In this Letter, we will study the propagating point dislocation in a 2D diffraction-free SPP field.

Nondiffracting beams, directional electromagnetic fields with minimum divergence within a certain propagation range, have found applications in optical trapping [9] and optical tomography [10] since Bessel beams were first introduced as a diffraction-free solution to free-space wave equations [11,12]. Free-space nondiffracting beams have already been used to study propagating screw dislocations in terms of high-order Bessel beams [13]. More recently, the concept of diffraction-free beams has been adopted in the 2D surface waves with the introduction of two types of nondiffracting SPPs: plasmonic Airy beams [14,15] and cosine-Gauss beams [16]. In this Letter, we aim to investigate the propagating point dislocations embedded in 2D diffraction-free cosine-Gauss beams.

We designed two phase-shifted SPP line sources to generate a singular SPP beam with a point dislocation at the center, which evolves into a straight diffraction-free dark channel along the propagation direction at the 2D air/metal interface. Figure 1(a) shows our design scheme: two SPP line sources [represented by parallel grooves in Fig. 1(b)] generate two SPP waves propagating normal to either set of grooves. These two SPP waves can be considered as plane waves when the length D of the grating is much larger than the effective wavelength of the SPP. In an analogy to an edge dislocation in free space, which is normally created by introducing a π phase shift over the two half-planes in the transverse dimension, in our design, one line source is half-a-cycle behind the other in phase [realized by a shift of half an SPP wavelength (λ_{sp}) in the position of the grating] to introduce a point dislocation (phase singularity) in the transverse dimension. The singular SPP beam is formed in the area where the two SPP plane waves overlap.

On a relatively thick silver film (120 nm in thickness), we designed gratings consisting of three grooves [Fig. 1(b)] to minimize the interference of the generated SPP waves with the illumination background by ensuring the intensity of

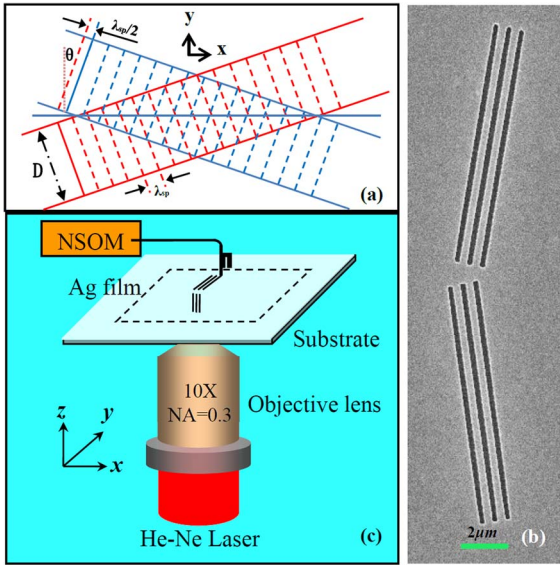


Fig. 1. (Color online) Schematic of singular SPP beam generation. (a) Two SPP plane waves are launched by two gratings with grooves of length D . The red dotted line behind the upper source (blue solid line) indicates the mirrored position of the lower plane-wave source (red solid line). We introduce a π phase shift over the two SPP sources by moving the upper SPP source along the propagating direction by $\lambda_{sp}/2$. The singular SPP beam is formed in the overlapping region of the two SPP plane waves. (b) Scanning electron microscopy (SEM) micrograph of the sample. D is $10\ \mu\text{m}$, and the tilted angle θ is 10° . The groove width is about $240\ \text{nm}$. (c) Experimental setup. The $633\ \text{nm}$ x -polarized Gaussian beam at normal incidence is slightly focused by an objective lens ($10\times$, $\text{NA} = 0.3$) onto the silver film. Aperture-type NSOM is used to map the near-field distributions of the SPP waves.

the generated SPP plane waves is much stronger than the partially transmitted free-space light. The silver film with grating structures is fabricated on top of an indium tin oxide ($10\ \text{nm}$ in thickness, used for the fabrication process) coated glass substrate by electron beam lithography followed by a lift-off process. To maximize the efficiency [17], the grating pitch is set to be equal to $\lambda_{sp} = 613\ \text{nm}$ for the incident $633\ \text{nm}$ laser. An aperture-type near-field scanning optical microscope (NSOM) (NT-MDT NTEGRA Solaris) with an aluminum coated fiber tip (tip aperture about $100\ \text{nm}$ in diameter) operated in the collection mode is used to map the intensity pattern of the singular SPP waves.

Figure 2(a) shows the finite-difference time-domain (FDTD) simulation results of SPP distributions with the parameters $D = 10\ \mu\text{m}$ and $\theta = 10^\circ$. The experimental result obtained by NSOM as shown in Fig. 2(b) is in good agreement with the full-wave calculations. To clearly see the point dislocation in the transverse dimension and diffraction-free properties of the singular plasmonic beam, we plotted the SPP intensity distributions at various propagation distances, and the results are given in Figs. 2(c) and 2(d). At the beam axis where the point dislocation situates, the FDTD calculated intensity approximately reaches zero, while the experimentally recorded intensity presents a minimum, which can be attributed to the finite aperture size of the NSOM probe and noises. The transverse intensity distribution remains almost invariant within a long propagation distance ($>40\ \mu\text{m}$), which clearly indicates the diffraction-free property of the singular SPP beam.

We further studied the point dislocation existing in the singular SPP beam by an interference experiment.

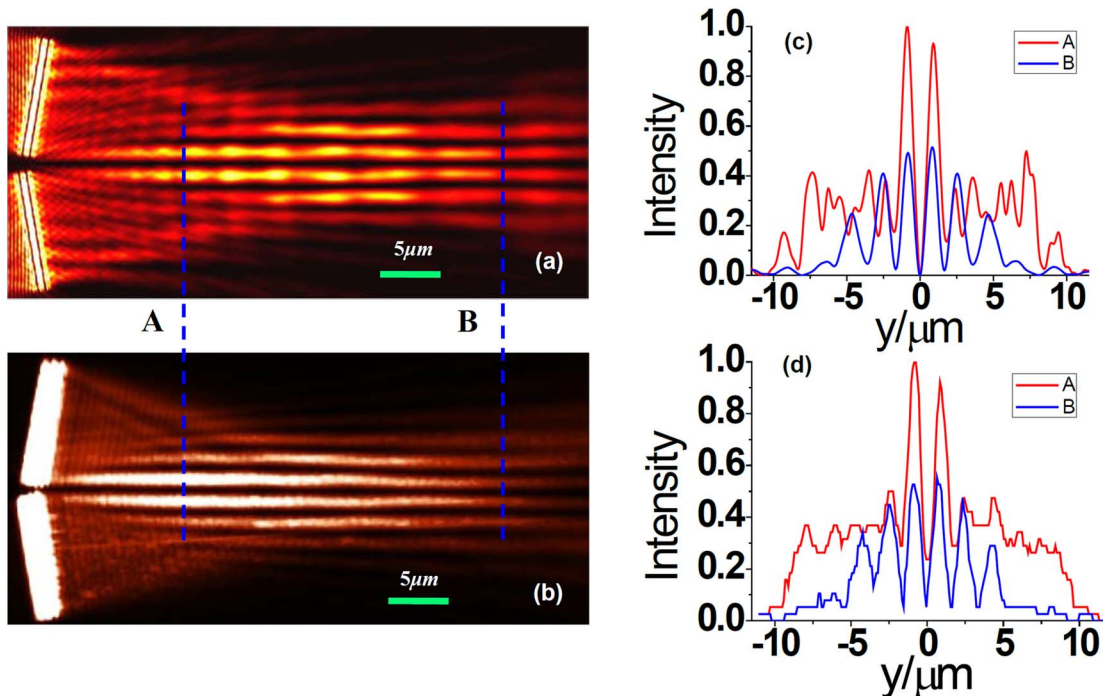


Fig. 2. (Color online) Singular SPP beam generated by two overlapped coupling gratings as shown in Fig. 1(b). (a), (b) Near-field intensity distributions obtained from (a) FDTD simulation and (b) NSOM measurement. (c), (d) Corresponding transverse intensity distributions at various propagation distances labeled by A and B in (a) and (b).

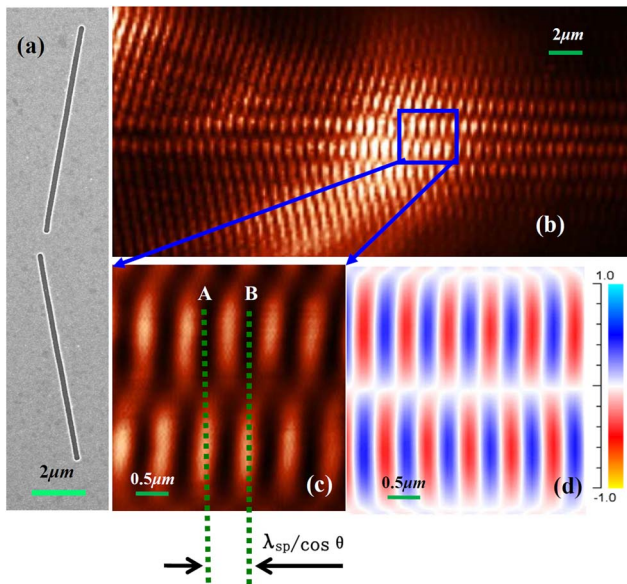


Fig. 3. (Color online) Point dislocation in a singular SPP beam. (a) SEM micrograph of a single-groove device. (b) Near-field intensity distribution obtained by NSOM. The fringes are formed by the interference between the singular SPP beam generated by a single-groove device and the background light. (c) Small region of the interference fringes outlined by the blue box in (b). At a specific propagation distance (labeled as A), the singular beam interferes with the transmitted light destructively in the upper part and constructively in the lower part. The period of fringes is defined as the distance between lines A and B, which matches the theoretical value $\lambda_{sp}/\cos\theta$. (d) Transient amplitude distribution obtained from FDTD calculation in the same region as in (c). The blue and red colors represent positive and negative values of the real part of the complex amplitude at a given moment, respectively. A π phase jump can be found across the singular line in the propagation axis.

As mentioned above, the intensity of SPP waves must be stronger than the intensity of partially transmitted light so that their interference can be neglected. However, we deliberately reduced the number of grooves to one [Fig. 3(a)], so the intensity of transmitted light is now comparable with that of the singular SPP wave. Figure 3(b) shows the near-field intensity pattern as a result of the interference between the singular SPP beam generated by the single-groove device and the transmitted light [18]. The pitch of the interference fringe is $\lambda_{sp}/\cos\theta = 622$ nm (620 nm as measured). The dislocation of interference fringes [Fig. 3(c)] indicates a π phase jump [Fig. 3(d)] along the phase singularity. The results indicate that the singular beam represents the antisymmetric modes in the family of cosine-Gauss beams.

In conclusion, we experimentally demonstrate a propagating point dislocation in a 2D space by mapping the near-field intensity distribution of the singular beam using NSOM. We also show in both full-wave calculations and interference experiments that the point dislocation

exists in the SPP beam. The singular beams could be used for nanophotonic applications, such as near-field optical signal transmission among next-generation on-chip devices [19] and plasmonic trapping of manipulation nanoparticles [20,21].

This work was partially supported by the National Natural Science Foundation of China under Grant Nos. 10974101, 61036013, and 61138003. XCY acknowledges the support given by the Ministry of Science and Technology of China under Grant No. 2002DFA52300 for China-Singapore collaborations, the National Research Foundation of Singapore under Grant No. NRF-G-CRP2007-01, and the Tianjin Municipal Science and Technology Commission under Grant No. 11JCZDJC15200. The authors thank Professor Haitao Liu for his invaluable discussions.

References

1. H. Raether, *Surface Plasmons on Smooth and Rough Surfaces and on Gratings* (Springer-Verlag, 1988).
2. L. Feng, K. A. Tetz, B. Slutsky, V. Lomakin, and Y. Fainman, *Appl. Phys. Lett.* **91**, 081101 (2007).
3. H. W. Gao, J. Henzie, and T. W. Odom, *Nano Lett.* **6**, 2104 (2006).
4. J. F. Nye and M. V. Berry, *Proc. R. Soc. Lond. Ser. A Math. Phys. Eng. Sci.* **336**, 165 (1974).
5. D. V. Petrov, *Opt. Commun.* **188**, 307 (2001).
6. H. Kim, J. Park, S. W. Cho, S. Y. Lee, M. Kang, and B. Lee, *Nano Lett.* **10**, 529 (2010).
7. P. S. Tan, G. H. Yuan, Q. Wang, N. Zhang, D. H. Zhang, and X.-C. Yuan, *Opt. Lett.* **36**, 3287 (2011).
8. V. E. Lembessis, M. Babiker, and D. L. Andrews, *Phys. Rev. A* **79**, 011806 (2009).
9. V. Garces-Chavez, D. McGloin, H. Melville, W. Sibbett, and K. Dholakia, *Nature* **419**, 145 (2002).
10. T. A. Planchon, L. Gao, D. E. Milkie, M. W. Davidson, J. A. Galbraith, C. G. Galbraith, and E. Betzig, *Nat. Methods* **8**, 417 (2011).
11. C. J. R. Sheppard and T. Wilson, *IEE J. Microwaves Opt. Acoust.* **2**, 105 (1978).
12. J. Durnin, J. J. Miceli, Jr., and J. H. Eberly, *Phys. Rev. Lett.* **58**, 1499 (1987).
13. J. Arlt and K. Dholakia, *Opt. Commun.* **177**, 297 (2000).
14. A. Minovich, A. E. Klein, N. Janunts, T. Pertsch, D. N. Neshev, and Y. S. Kivshar, *Phys. Rev. Lett.* **107**, 116802 (2011).
15. L. Li, T. Li, S. M. Wang, C. Zhang, and S. N. Zhu, *Phys. Rev. Lett.* **107**, 126804 (2011).
16. J. Lin, J. Dellinger, P. Genevet, B. Cluzel, F. de Founel, and F. Capasso, *Phys. Rev. Lett.* **109**, 093904 (2012).
17. B. Lee, S. Kim, H. Kim, and Y. Lim, *Prog. Quantum Electron.* **34**, 47 (2010).
18. B. Wang, L. Aigouy, E. Bourhis, J. Gierak, J. P. Hugonin, and P. Lalanne, *Appl. Phys. Lett.* **94**, 011114 (2009).
19. E. Ozbay, *Science* **311**, 189 (2006).
20. M. Righini, G. Volpe, C. Girard, D. Petrov, and R. Quidant, *Phys. Rev. Lett.* **100**, 186804 (2008).
21. K. Wang, E. Schonbrun, P. Steinvurzel, and K. B. Crozier, *Nano Lett.* **10**, 3506 (2010).